Optimum Particle Size for Seeding Convective Clouds

Yan YIN

Nanjing University of Information Science and Technology (NUIST), Nanjing, China
yinyan@nuist.edu.cn

- What kind of chemicals can be used for hygroscopic seeding? Why?
- What size of particles should be used in order for an optimum seeding effect?
- What kind of numerical models should be used for simulations of hygroscopic seeding?

OUTLINE

- Particle sizes used in classical seeding practice
- Particles sizes from hygroscopic flares
- Modeling of hygroscopic seeding
- Recommendations for optimum particle size for seeding convective clouds

Particle sizes used in classical seeding practice

- In classical hygroscopic seeding experiments, particles with the diameter larger than 10 μm are used to provide embryonic raindrops
- Both seeding below cloud base and at cloud top are tested
- NaCl, CaCl, NH_4NO_3, NH_2CONH_2 (urea) are the common seeding agents
- The disadvantages of this method including: the large quantity of seeding material, inconvenient to handle, and the adverse effect to the environment

Particle sizes used in classical seeding practice

- Hygroscopic seeding in China:
  - Start from the late 1950s
  - Seeding at cloud top with giant salt particles or ground based burning of hygroscopic materials
  - ~7% increase in rain amount

Recent advances in hygroscopic seeding

- Hygroscopic flares which mainly consist of KCl, NaCl, MgO, $LiCO_3$ are used in South Africa
- The seeding particles produced from burning of flares with a broad spectrum with the mean size of 0.5 μm
- Mexico Coahuila project repeated South African's method (WMO, 2000)

Hygroscopic Seeding in South Africa

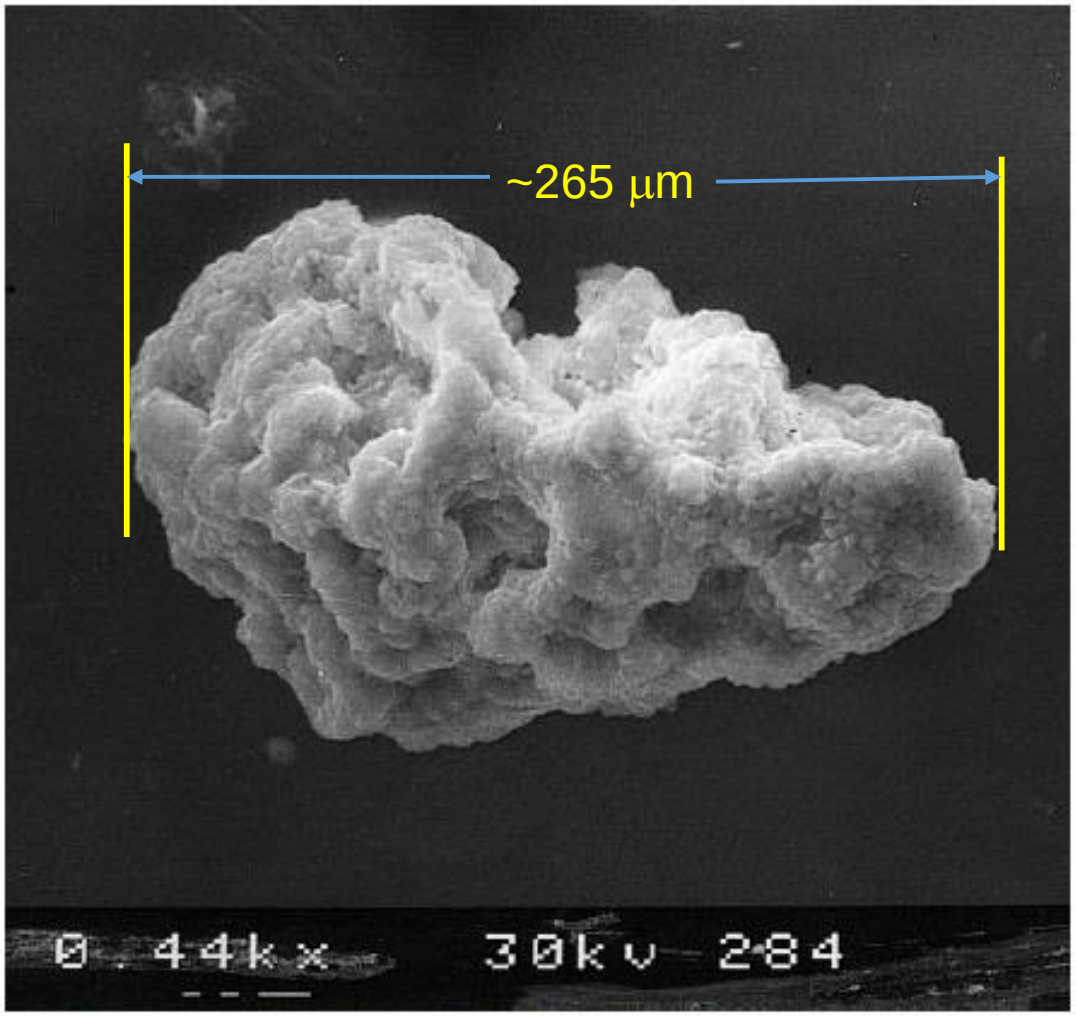

FIG. 8. Electron microscope photograph of a large particle collected on a sticky slide held in the plume of a flare burning on the seeding aircraft on the ground with engines running. Horizontal dimension of this particle is about 165 μm.

A giant particle produced from combustion of flares (Mather et al., 1997)

Hygroscopic Seeding in South Africa

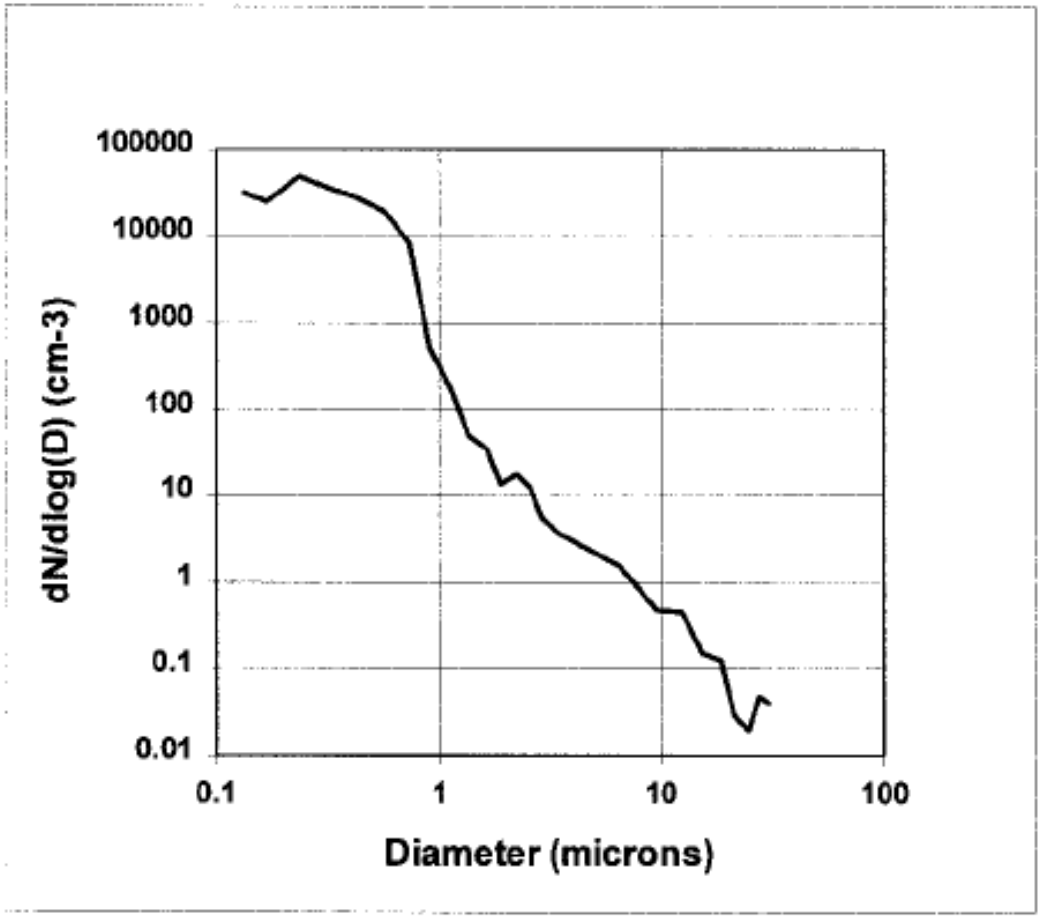

FIG. 7. Dry particle spectrum of combustion products from the hygroscopic seeding flare measured by an instrumented aircraft flying 50 m in trail behind the seeding aircraft using a PCASP-100X and an FSSP-100 probe.

Particle spectrum produced from combustion of flares (Mather et al., 1997)

Hygroscopic Seeding: droplet size distribution

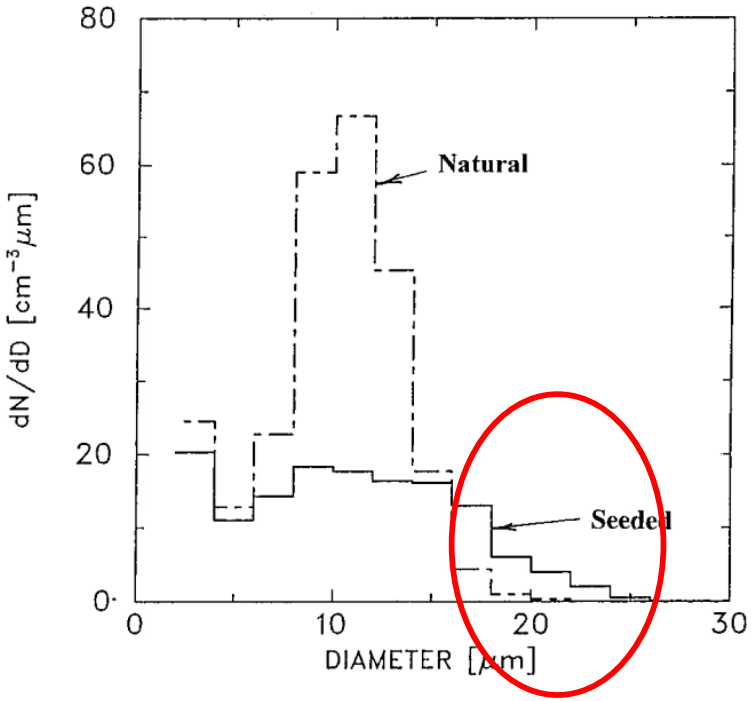

	Seeded	Natural
Time (SAST):	14:12:42	14:12:55
Liquid Water (g/kg):	0.33	0.35
Concentrations (cm^{-3}):	280	508

South Africa:

The hygroscopic seeding at cloud base accelerates the growth of large hydrometeors in the treated clouds, which harvest more of the available supercooled water before it is expelled into the anvils by the strong updrafts that are a characteristic of the local storms, thereby increasing the *efficiency* of the rainfall process.

FIG. 9. Droplet size distributions measured about 200 m above cloud base in a seeded cloud. The dashed curve shows an example of the typical size distribution observed in most of the cloud, and thought to be natural. The solid line distribution, measured in the same cloud, is believed to be in the seeded portion of the cloud. The Learjet remained in the seeded portion of this cloud for a total of 3 s.

Mather et al. (1997)

Recent advances in hygroscopic seeding

- Randomized hygroscopic seeding in Thailand (Silverman et al., 2000):
  - 1995-1998 in Bhumibol region of northwest Thailand, 4 hygroscopic materials are used to seed tropical convective clouds, including NaCl, CaCl, NH_4NO_3, NH_2CONH_2 (urea)
  - The most important finding:
    - CaCl is the best seeding material
    - Optimum size: 10~30μm in radius
    - Seeding near cloud base is better than at cloud top
    - Seeding effects are positively correlated with seeding amount
    - The optimum seeding time is before a clear radar echo from weather radar

Modeling of hygroscopic Seeding

Parcel model

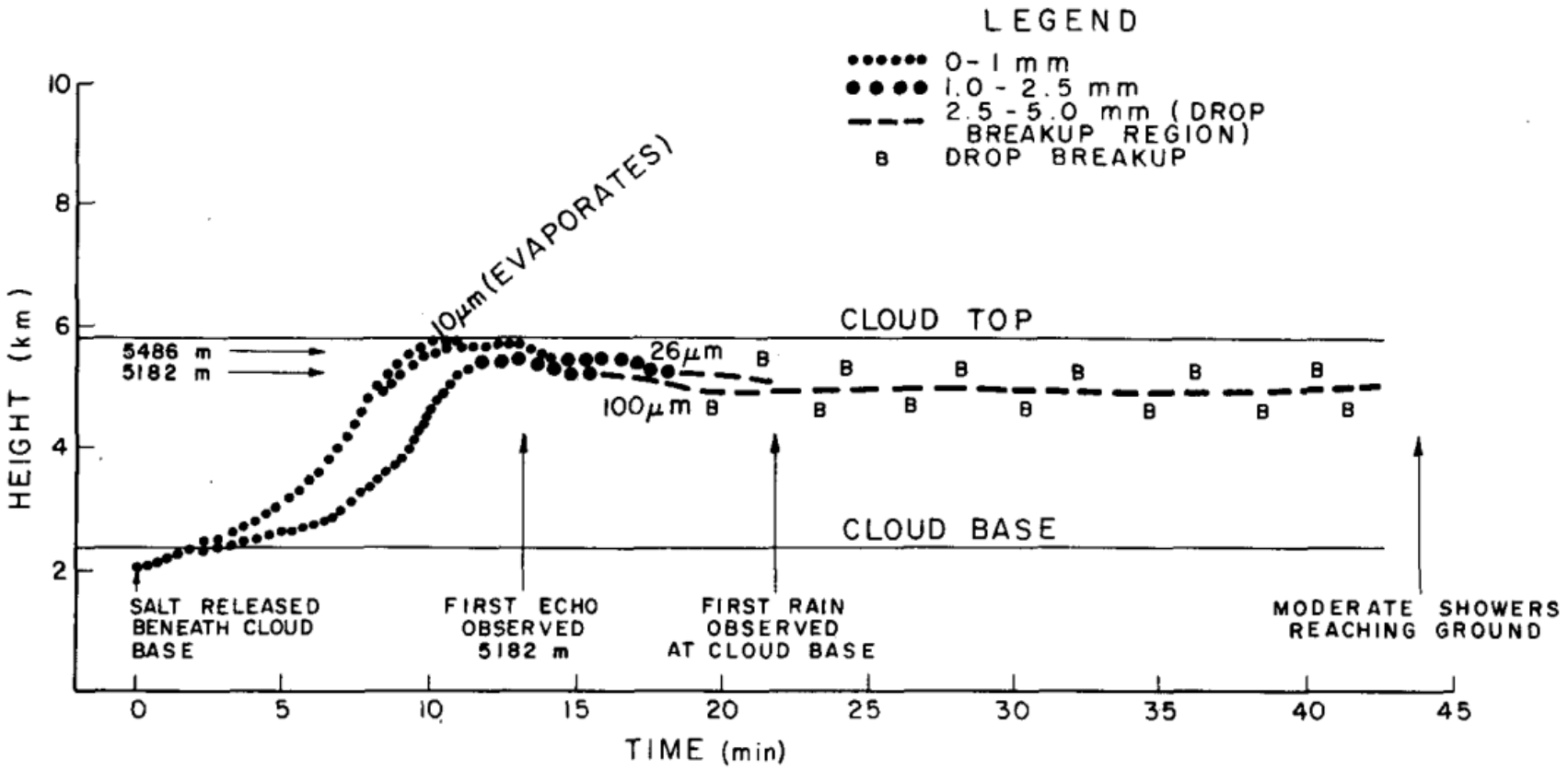

FIG. 9. Condensation-coalescence model computations of the growth pattern and trajectory of three different sized salt particles released beneath the base of a cloud whose physical characteristics are believed to be similar to a real cloud system that was stimulated to rain through salt seeding. See text for discussion.

Klazura and Todd (1978)

Hygroscopic Seeding: droplet size distribution

Parcel model

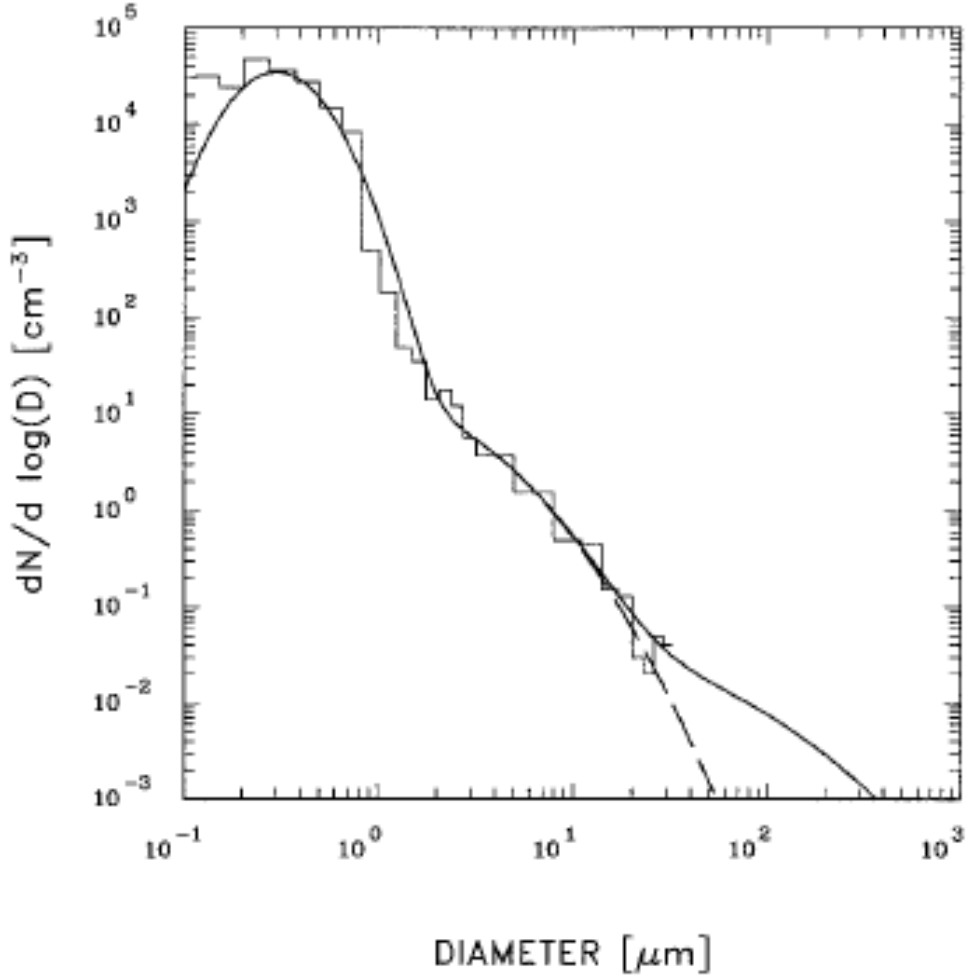

FIG. 1. Size distribution of particles measured at a distance of about 50 m behind the seeding aircraft, during in-trail flight in dry air (with relative humidity of about 30%). The smooth solid curve is the sum of three lognormal distributions, as described in the text; the dashed curve is based on all but the largest lognormal component.

Cooper et al. (1997)

Hygroscopic Seeding: particle size distribution

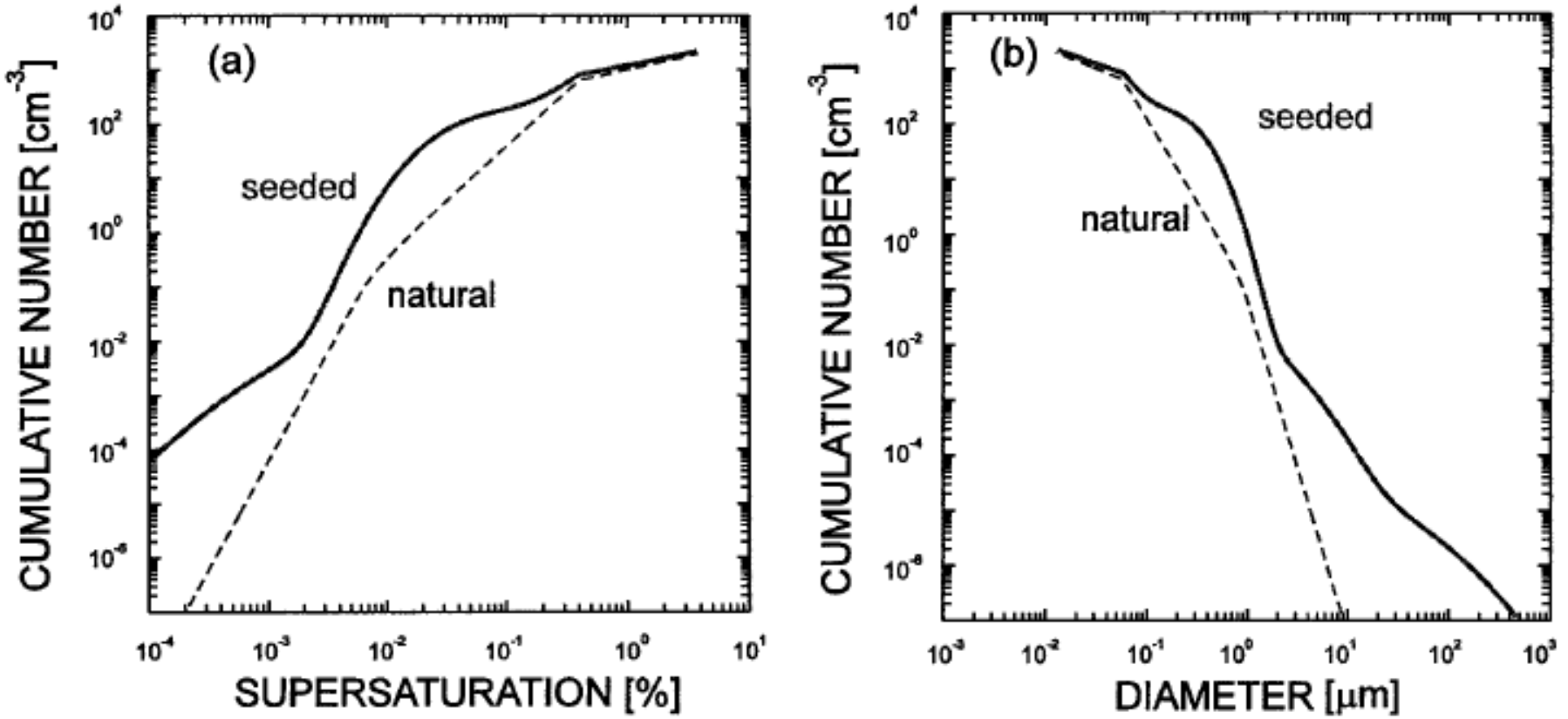

FIG. 3. (a) Cumulative concentration of CCN as a function of supersaturation for natural and seeded cases representing continental conditions. The corresponding size distribution is shown in Fig. 3b. (b) Cumulative size distribution of soluble particles (ammonium sulfate) corresponding to the CCN activity distributions of Fig. 3a.

Cooper et al. (1997)

Hygroscopic Seeding: droplet size distribution

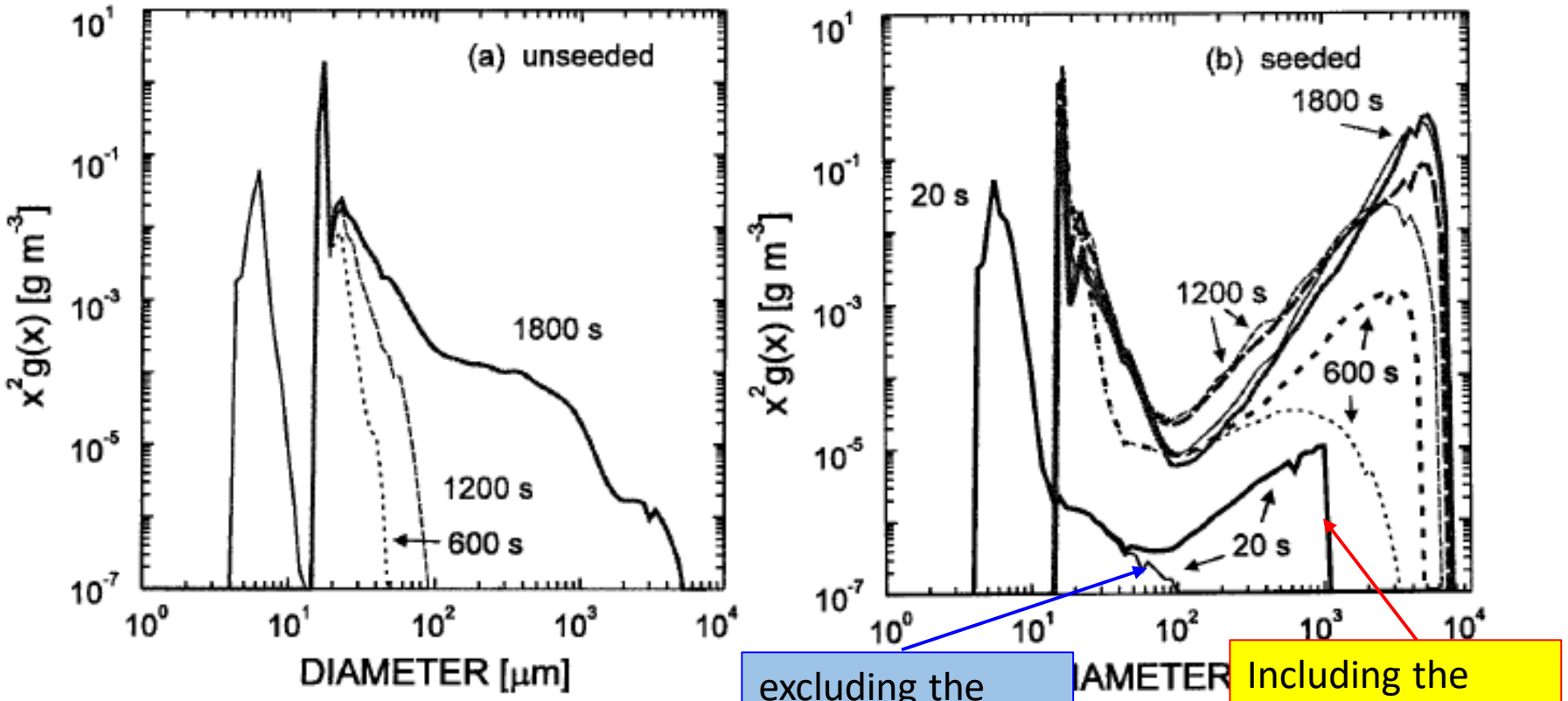

FIG. 4. (a) The mass distribution functions 20, 600 (dotted line),1 after passage for the unseeded case. The distribution function $g(x)$ (where x is t ghted by $x2$ to show the distribution of liquid water content with the logarithm of mass. The true abscissa for this distribution function is mass x, but the abscissa is labeled here in terms of equivalent droplet diameter. The ordinate in these plots is equal to one-third of the distribution function $g(\ln r)$ used by Berry and Rinehardt (1974a, b) to display the liquid water content. (b) Mass distribution functions, as in Fig. 4a, for the seeded case. The two curves shown for each time represent the two different size distributions shown in Fig. 1, the thin lines excluding the largest particles and the thick lines including those particles.

Cooper et al. (1997)

Hygroscopic Seeding: droplet size distribution

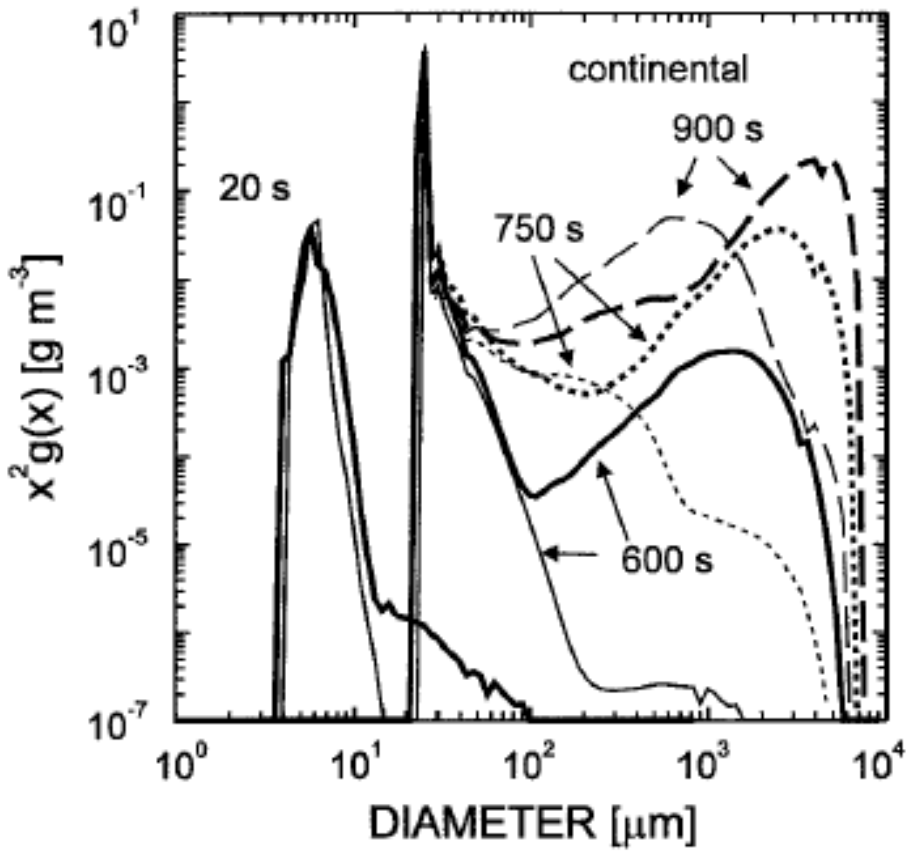

FIG. 8. Mass distribution functions, as in Fig. 4, showing the results of condensation and coalescence for the continental case, after 20, 600, 750, and 900 s of calculation. The solid lines denote results for 20 s and 600 s, the short-dashed lines denote results for 750 s, and the long-dashed lines denote results for 900 s; thin lines are the results for the control case, and thick lines are for the seeded case.

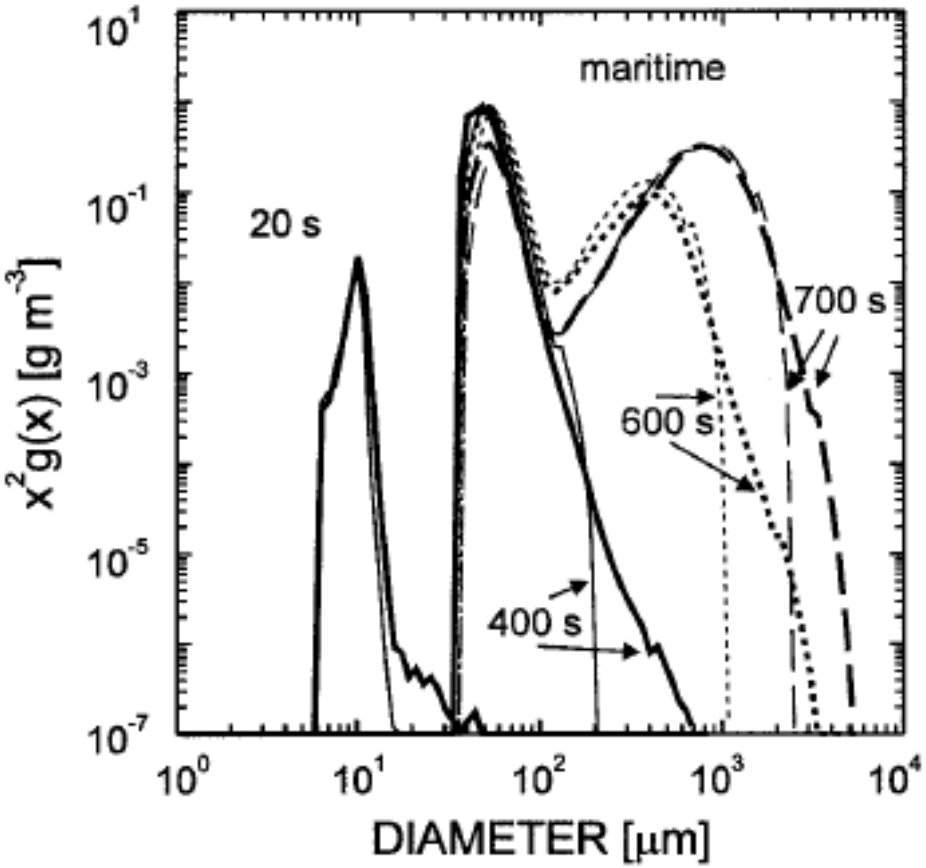

FIG. 10. Mass distribution functions, as in Fig. 8, showing the results of condensation and coalescence for the seeded (thick lines) and control (thin lines) maritime cases, after 20, 400, 600, and 700 s of growth.

Cooper et al. (1997)

Hygroscopic Seeding: droplet size distribution

- The particles having diameters near 0.3 μm apparently did not have beneficial effects and, in some cases, inhibited precipitation formation.
- However, increasing the mean size to about 0.5 μm led to positive effects in all cases, and a mean size of 1.0 μm was very effective while increasing the production of drizzle dramatically.

Cooper et al. (1997)

Hygroscopic Seeding: droplet size distribution

In order to realistically simulate the response of cloud microphysical properties to hygroscopic seeding, BIN microphysical cloud models are needed!

Hygroscopic Seeding: droplet size distribution

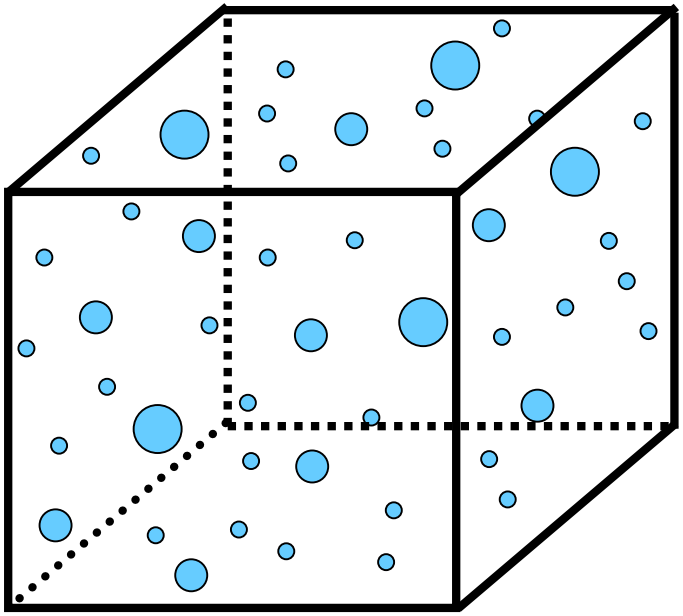

1 m³
(unit volume)

[e.g. Cloud droplets]

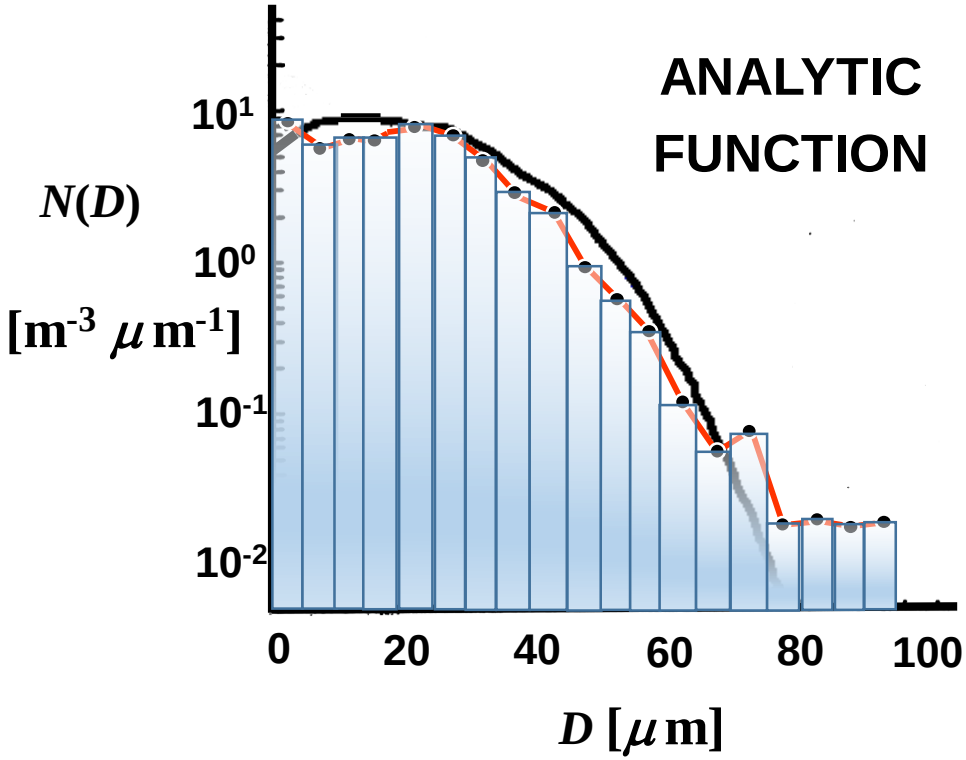

Milbrandt and Yau (2004)

The Model

- A dynamic cloud model with bin-resolved microphysics and chemistry
- Warm rain processes: drop activation, condensation/evaporation, collision-coalescence or breakup, sedimentation
- Ice-phase processes: ice nucleation (deposition, condensation-freezing, contact nucleation, and immersion freezing), ice multiplication, deposition and sublimation of ice particles, ice-ice and ice-drop interactions, melting of ice particles and sedimentation
- Aerosol scavenging: nucleation scavenging and impaction scavenging due to Brownian diffusion, inertia, hydrodynamic and phoretic forces
- Gas scavenging: A kinetic module of gas uptake by hydrometeors
- Chemistry: sulfur chemistry at present
- Two moments for aerosols and hydrometeors(drop, ice crystal, graupel and snow)
- 34 bins for hydrometeors and 43 bins for aerosols

(Yin et al. 2000, 2005)

Modeling of Hygroscopic Seeding

2D bin model

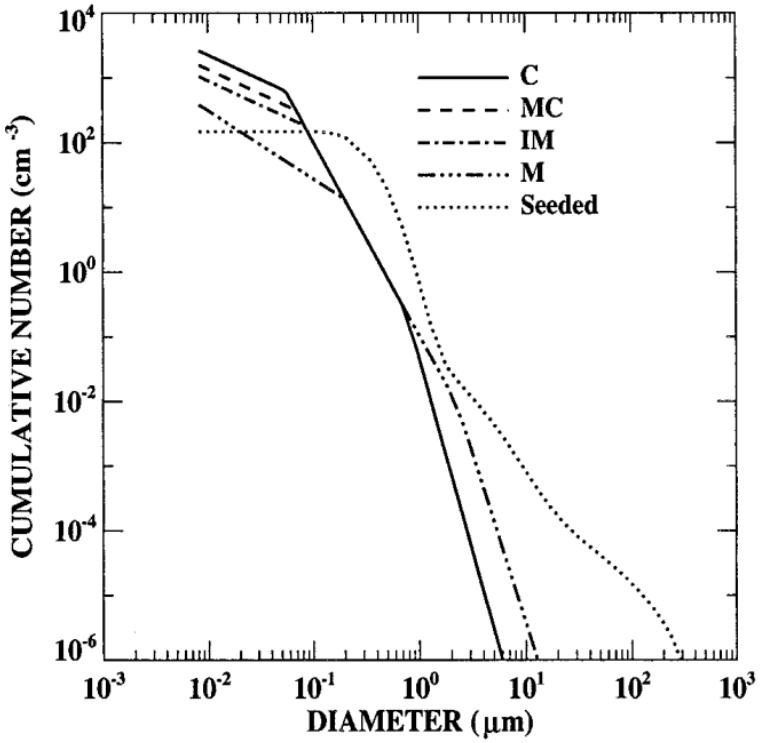

FIG. 2. Distributions of initial CCN and seeded particles from the flares. See text for a more detailed explanation.

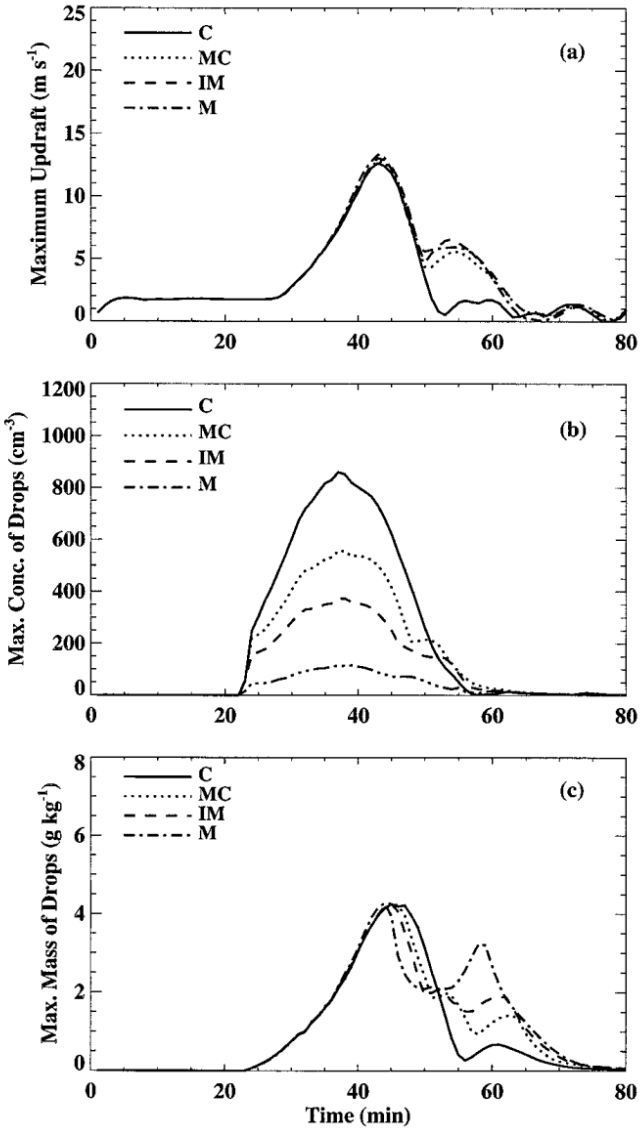

FIG. 3. Maximum values of (a) updraft speed, (b) droplet concentration, and (c) LWC at the middle axis as a function of time in clouds formed on different CCN spectra.

Yin et al. (2000)

Hygroscopic Seeding: droplet size distribution

TABLE 3. Seeding parameters and differences between the seeded and unseeded clouds in accumulated rain at the middle of domain ΔR_{ac}, integrated rain amount ΔR_{int}, and time of rain intiation T_r.

Case	Particle size (μm)	Seeding amounts	Time (min)	Height (km)	ΔR_{ac} (%)	ΔR_{int} (%)	T_r (min)
C1	Full	150 cm^{-3}	2–6	1.5	96.1	8.6	45
C2	Full	150 cm^{-3}	6–10	1.5	125.2	17.9	45
C3	Full	150 cm^{-3}	10–14	1.5	72.8	11.7	47
C4	Full	150 cm^{-3}	14–18	1.5	14.6	0.7	49
C5	Full	150 cm^{-3}	18–22	1.5	0.0	−0.4	55
C6	$1 \le r \le 10$	26.7 L^{-1}	6–10	1.5	0.0	0.1	55
C7	$r \ge 10$	0.16 L^{-1}	6–10	1.5	136.9	33.7	45
C8	$r \le 1$	150 cm^{-3}	6–10	1.5	−12.6	−17.1	55
C9	Full	150 cm^{-3}	6–10	1.8	204.9	29.8	43
C10	Full	150 cm^{-3}	6–10	2.1	255.3	40.4	42
C11	$r \ge 10$	0.16 L^{-1}	6–10	2.1	288.4	66.3	42
C12	Full	750 cm^{-3}	6–10	1.5	337.9	48.5	41
C13	Full	1500 cm^{-3}	6–10	1.5	508.7	89.7	41
C14	$r \ge 10$	1.6 L^{-1}	6–10	1.5	592.2	162.1	41
C15	$1 \le r \le 10$	2.67 cm^{-3}	6–10	1.8	149.5	107.5	51
C16	$r \ge 10$	0.45 L^{-1}	6–10	1.8	546.5	131.5	40
MC1	Full	150 cm^{-3}	2–6	1.5	−1.0	−16.0	45
MC2	Full	150 cm^{-3}	6–10	1.5	−1.2	−15.8	45
MC3	Full	150 cm^{-3}	10–14	1.5	−2.4	−9.2	47
MC4	Full	150 cm^{-3}	14–18	1.5	−7.0	−5.9	50
MC5	Full	150 cm^{-3}	18–22	1.5	−2.6	−1.6	53
MC6	$1 \le r \le 10$	26.7 L^{-1}	6–10	1.5	0.0	0.1	53
MC7	$r \ge 10$	0.16 L^{-1}	6–10	1.5	31.9	4.3	45
MC8	$r \le 1$	150 cm^{-3}	6–10	1.5	−29.7	−22.2	53
IM1	Full	150 cm^{-3}	6–10	1.5	3.0	−12.1	45
IM2	$r \ge 10$	0.16 L^{-1}	6–10	1.5	14.1	0.3	45
M1	Full	150 cm^{-3}	6–10	1.5	−3.7	−3.4	45
M2	$r \ge 10$	0.16 L^{-1}	6–10	1.5	2.8	0.0	45

Seeding time

Particle size

altitude

Seeding amount

Yin et al. (2000)

Hygroscopic Seeding: droplet size distribution

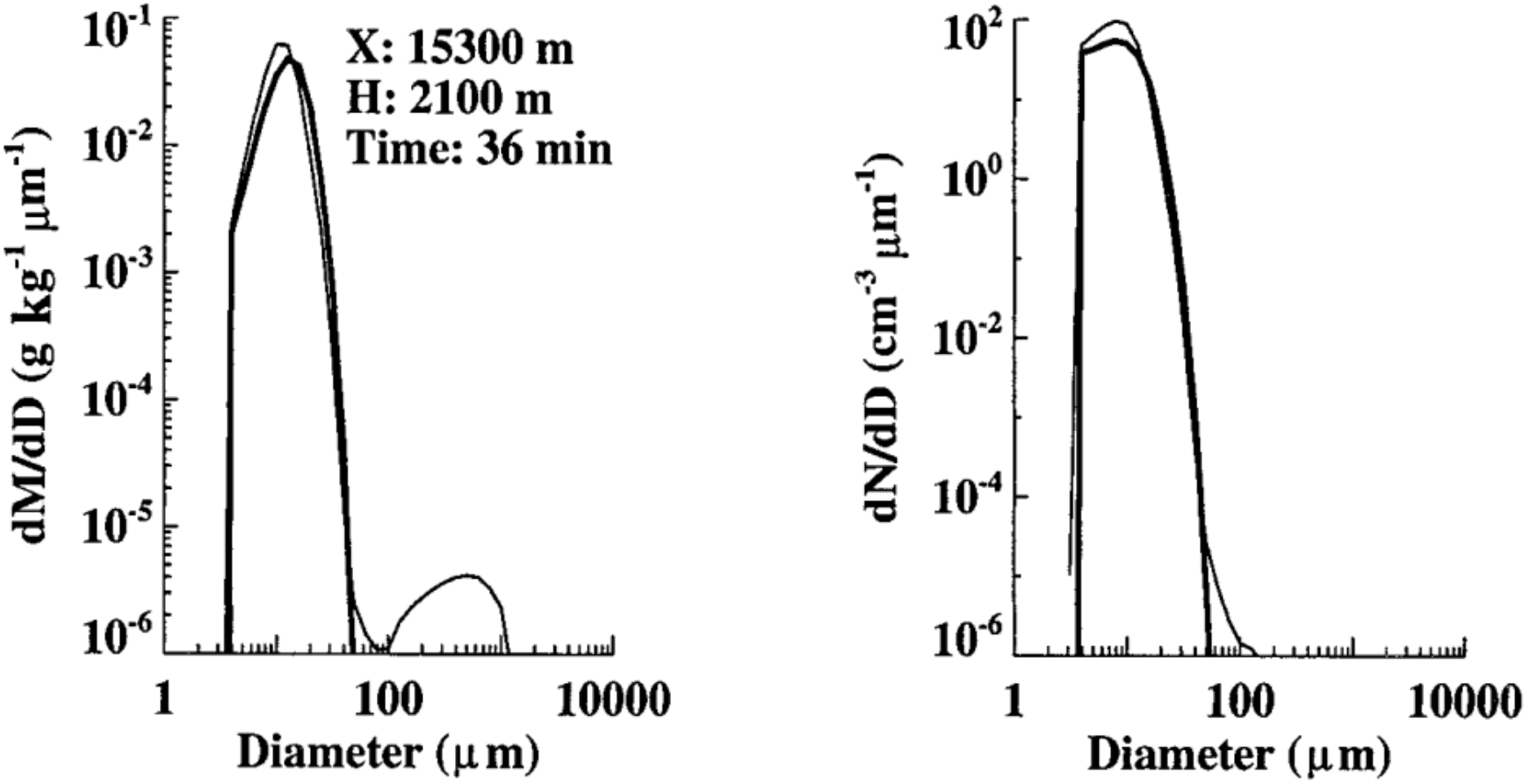

FIG. 4. Drop mass (left) and concentration (right) distributions for the unseeded case C0 (thick line) and seeded case C2 (thin line) after 36 min of simulation. The location is shown above the curves.

Yin et al. (2000)

Hygroscopic Seeding: droplet size distribution

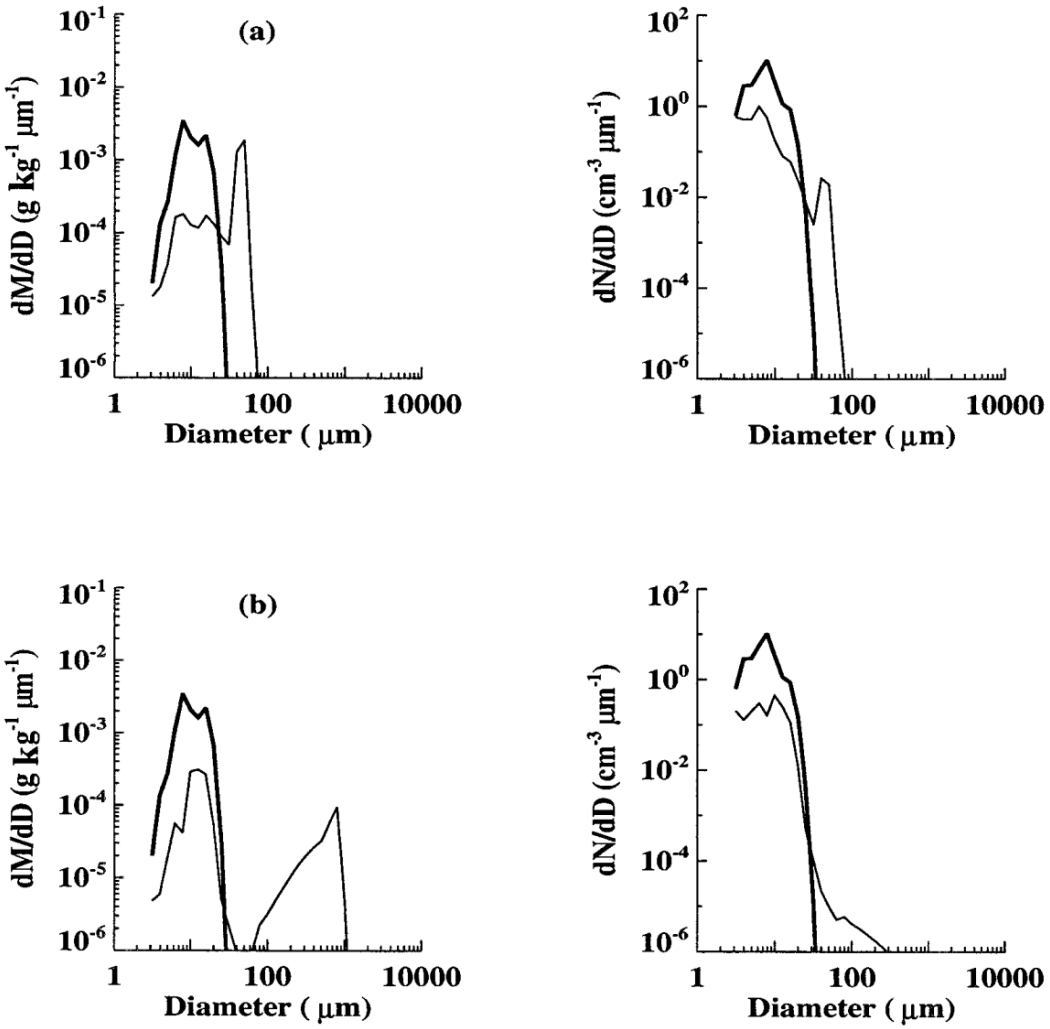

FIG. 8. Droplet mass and concentration distributions at cloud base for the unseeded case (thick line) and seeded case (thin line), 1 min after completing seeding. (a) C0 vs C15; (b) C0 vs C16.

Yin et al. (2000)

Hygroscopic Seeding: droplet size distribution

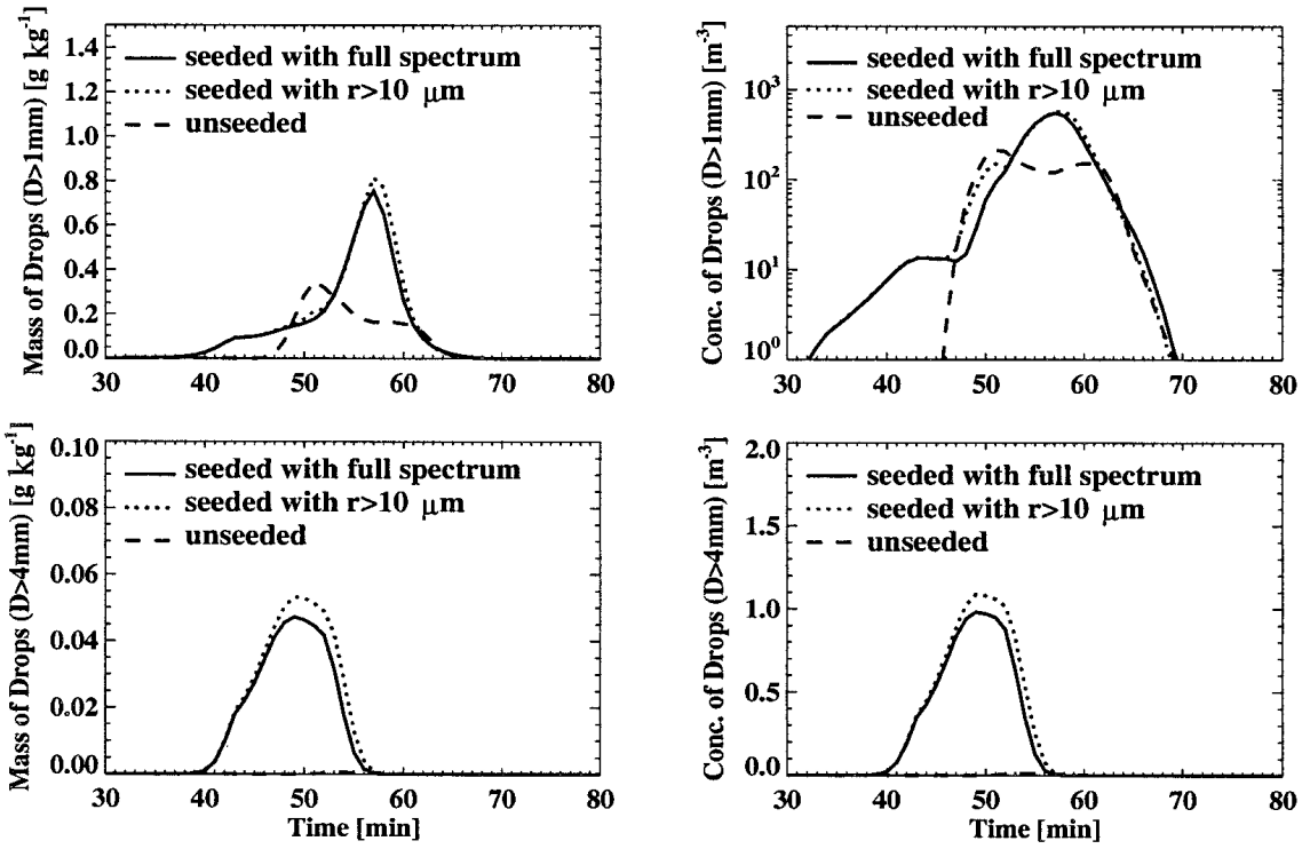

FIG. 7. Maximum values of water content (left) and concentration (right) of the raindrops with diameter larger than 1 (top) and 4 mm (bottom), respectively, in the unseeded case (dashed line), the case seeded with the full spectrum of particles from the flares (solid line), and the case seeded with only particles larger than 10 μm (dotted line).

Yin et al. (2000)

Hygroscopic Seeding: precipitation

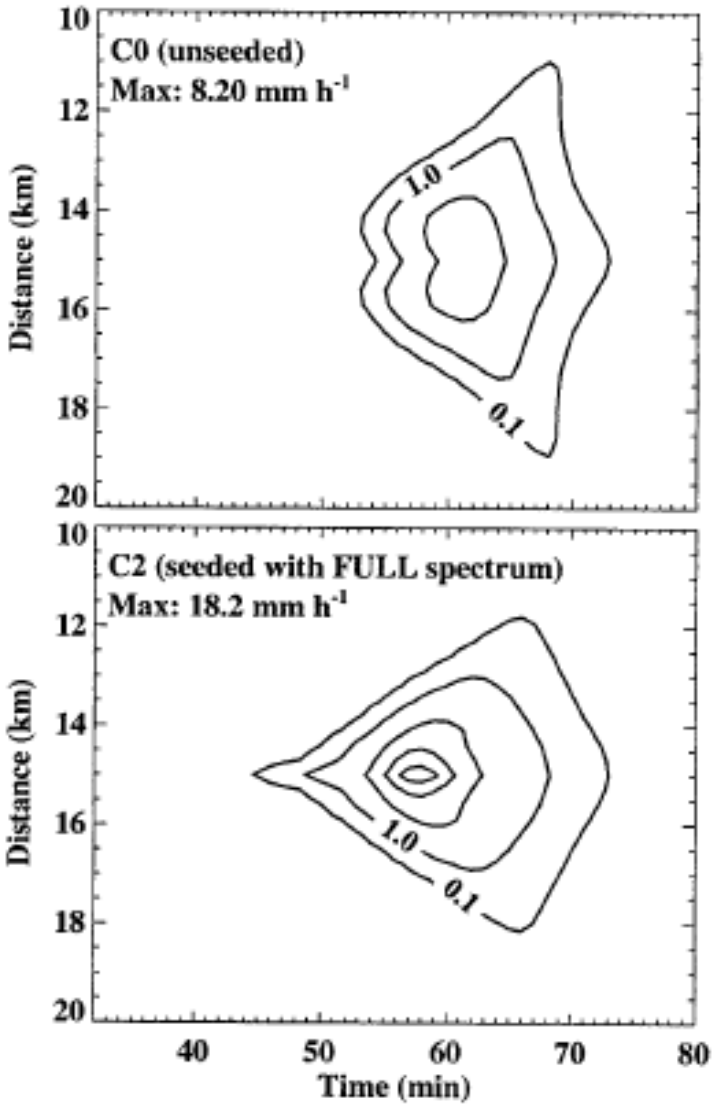

FIG. 6. Rainfall rate on the ground as a function of time in the unseeded case (top) and seeded case (C2; bottom). The contours are 0.1, 1, 5, 10, 15 mm h^{-1}.

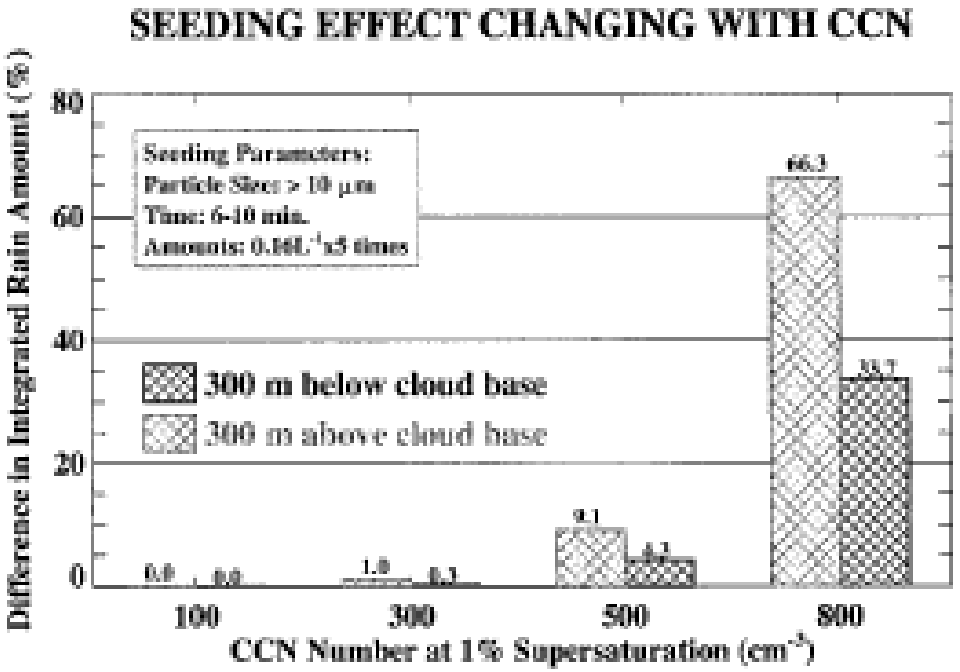

FIG. 9. Differences in integrated rain amount between the seeded and unseeded cases for clouds with different natural CCN.

Yin et al. (2000)

Hygroscopic Seeding: conclusions

- Out of the full spectrum, the most effective particles were those with radii larger than 1 μm, especially those larger than 10 μm; the particles smaller than 1 μm always had a negative effect on the rain development.
- The biggest precipitation enhancement was obtained when seeding was conducted a few minutes after cloud initiation and above cloud base. The radar reflectivity at that time period was lower than 0 dBZ.
- Rain enhancement also increased with the increase in the concentration of the large seeding particles in the spectrum

Yin et al. (2000)

Hygroscopic Seeding: droplet size distribution

Parcel model

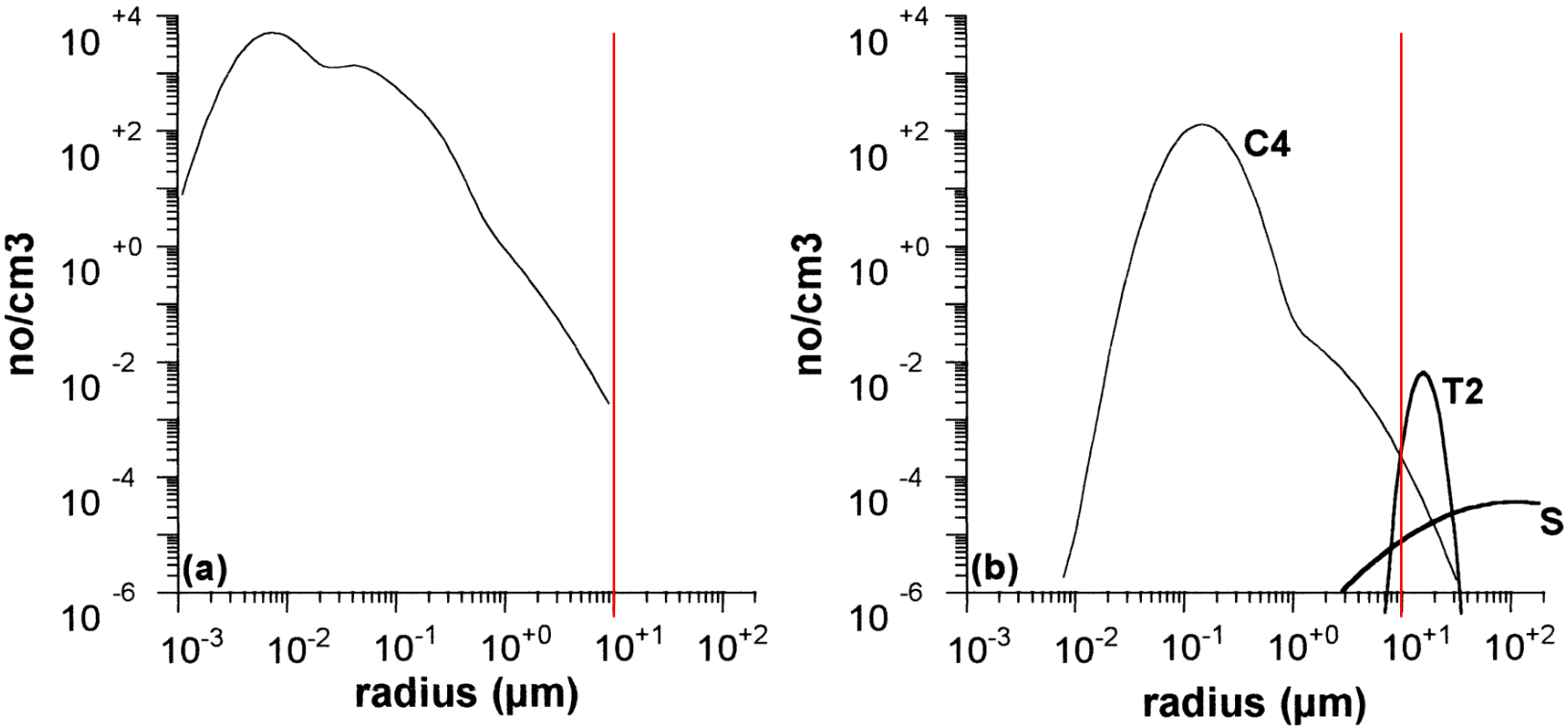

FIG. 1. (a) Initial dry number density distribution function of the background aerosol particle spectrum as given by Eq. (1) and Table 2. (b) Initial dry number density distribution function of the seeding aerosol particle spectrum after CBM97 (C4), TRL94 (T2), and SS96 (S).

Caro et al. (2002)

Hygroscopic Seeding: droplet size distribution

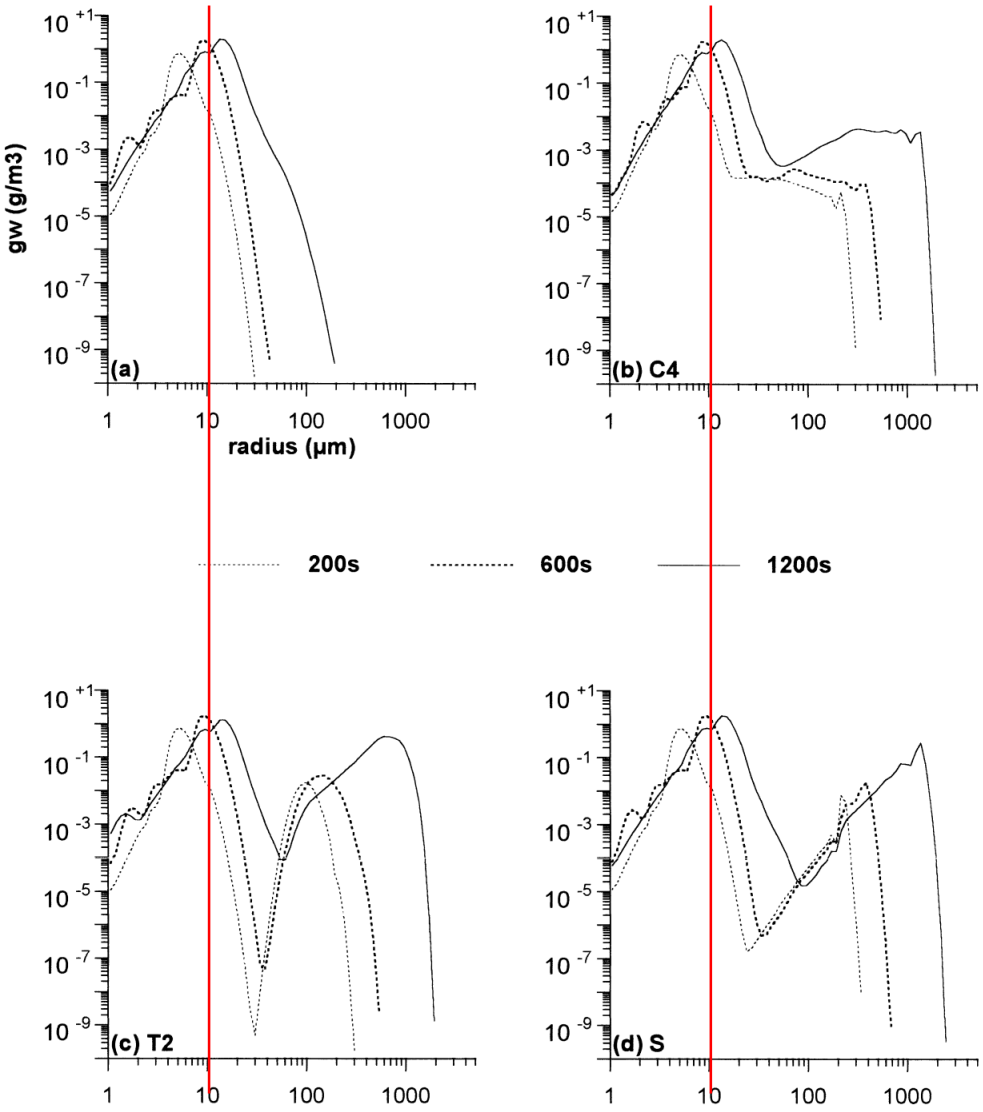

FIG. 2. Drop water mass density distribution function as a function of drop radius and as a function of parcel lifetime (a) for the unseeded case, (b) for case C4 (c), for case T2 and, (d) for case S, for a warm convective cloud, for an entrainment rate of $\alpha = 0.6$.

Caro et al. (2002)

Hygroscopic Seeding: collection process

1D model with TiO2/NaCl

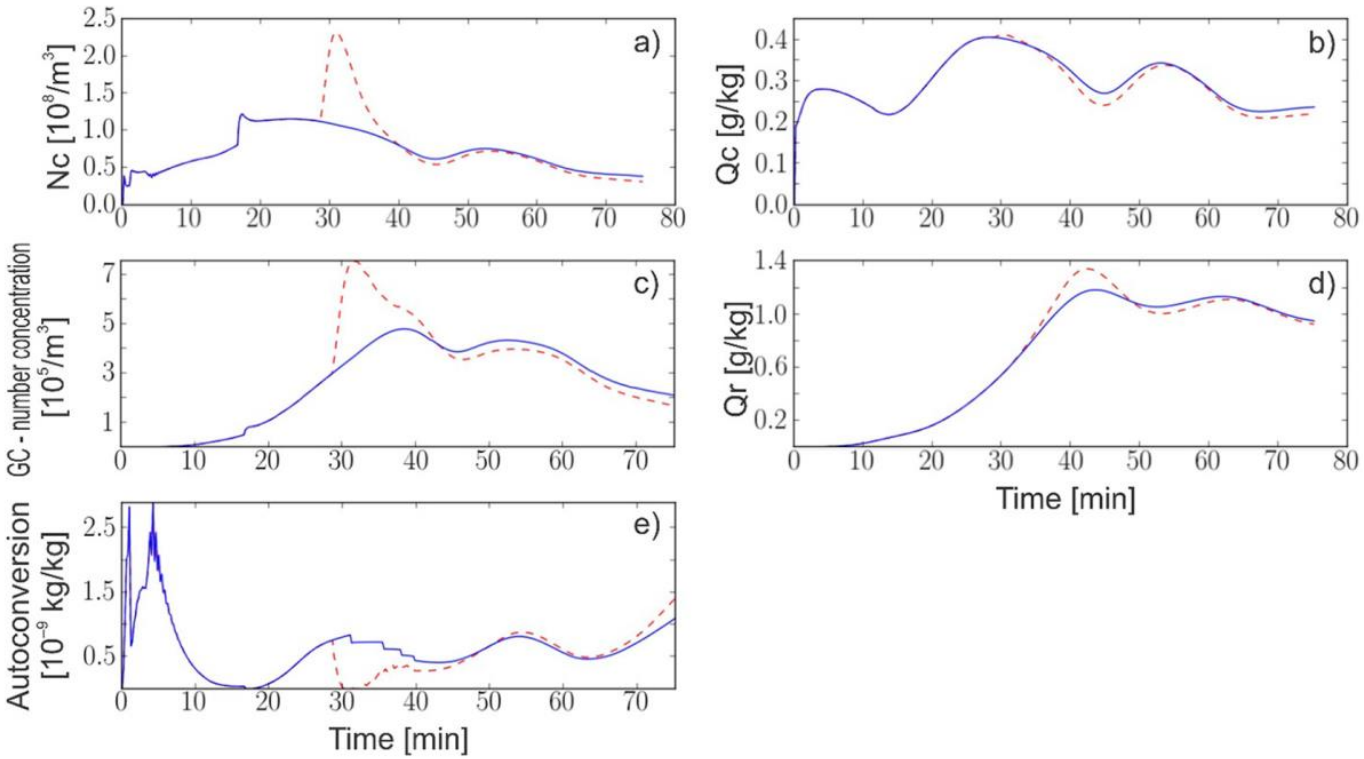

Fig. 8. Evolution of different characteristics of cloud water (subscript c), rain water (subscript r), autoconversion and gravitational collection in 75 min of simulation with MSCE 1D model. The blue (full) lines represent the unseeded case and the red (dashed) lines correspond to the seeded case (shell structured TiO_2/NaCl). These results correspond to the height of 2000 m above the lower cloud base. (For interpretation of the references to colour in this figure legend, the reader is referred to the web version of this article.)

Lompar et al. (2018)

Hygroscopic Seeding: collection process

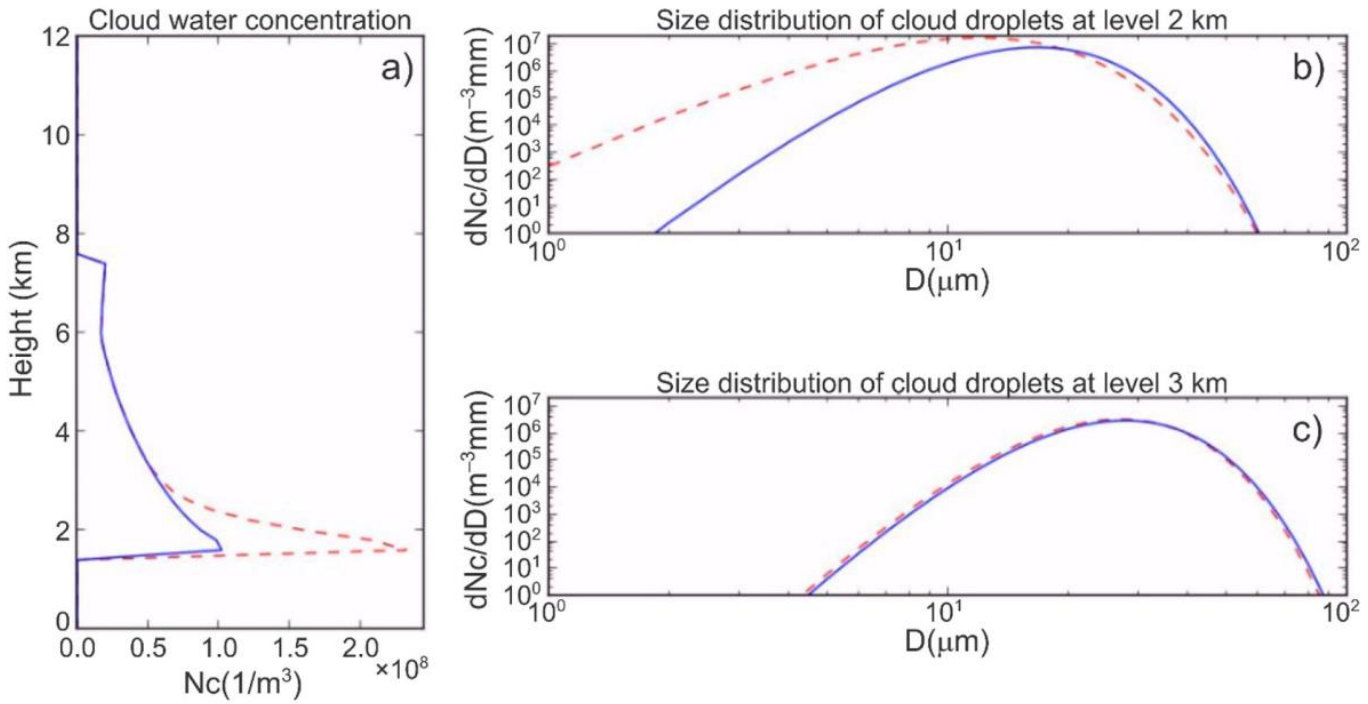

Fig. 9. (a) Vertical profile of cloud droplet concentration at $t = 28$ min for natural (blue) and novel (red) aerosols and their size distributions at clod base (b) and 1 km above cloud base (c). (For interpretation of the references to colour in this figure legend, the reader is referred to the web version of this article.)

Lompar et al. (2018)

Hygroscopic Seeding: collection process

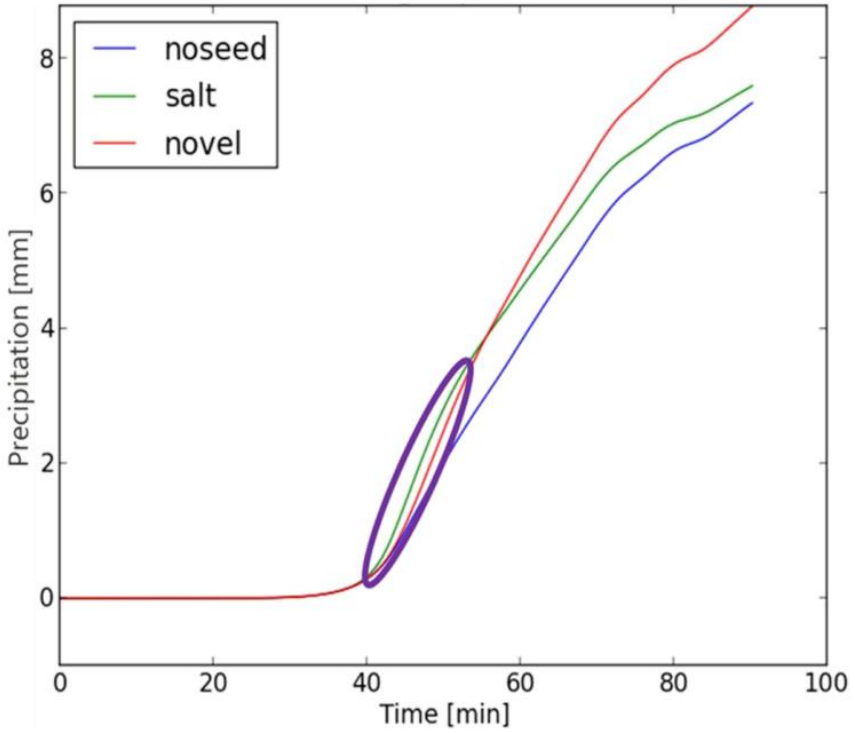

Fig. 10. Evolution of the accumulated surface precipitation for the unseeded case (blue) and two seeded cases: (1) pure NaCl (green), and (2) shell structured TiO_2/NaCl (red). (For interpretation of the references to colour in this figure legend, the reader is referred to the web version of this article.)

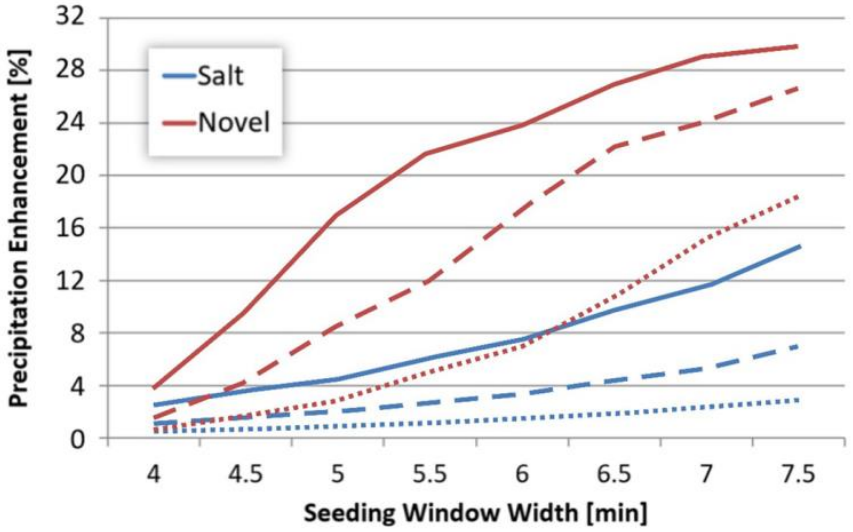

Fig. 11. Precipitation enhancement as a function of spatiotemporal windows for pure NaCl (blue) and shell structured TiO_2/NaCl (red) aerosols. The seeded particles are injected at 200 m (full lines), 400 m (dashed lines) and 600 m (dotted lines) levels. See text for more details. (For interpretation of the references to colour in this figure legend, the reader is referred to the web version of this article.)

Lompar et al. (2018)

Summery

- Hygroscopic Seeding in clouds alters the initial cloud droplet spectrum, and affects the condensational growth and effective radius of droplets.
- The changes in effective radius impacts the collision-coalescence of large drops, and hence change the rain rate and spatial distribution of precipitation.
- The seeding effects on cloud macro- and microphysical processes can be different with varied background aerosol concentration, seeding spectrum, atmospheric humidity, wind shear, etc.

Recommendations for seeding convective clouds

- Hygroscopic Seeding in clouds alters the initial cloud droplet spectrum, and affects the condensational growth and effective radius of droplets.
- The changes in effective radius impacts the collision-coalescence of large drops, and hence change the rain rate and spatial distribution of precipitation.
- The seeding effects on cloud macro- and microphysical processes can be different with varied background aerosol concentration, seeding spectrum, atmospheric humidity, wind shear, etc.

Any Questions?